



ORIGINAL ARTICLE OPEN ACCESS

Establishment of a Novel Caco-2-Based Cell Culture System for Human Sapovirus Propagation

Yuya Fukuda^{1,2}  | Azusa Ishikawa¹ | Ryoka Ishiyama¹ | Reiko Takai-Todaka¹ | Kei Haga¹ | Yuichi Someya³ | Tomomi Kimura-Someya⁴ | Kazuhiko Katayama¹ 

¹Laboratory of Viral Infection Control, Department of Infection Control and Immunology, Ōmura Satoshi Memorial Institute & Graduate School of Infection Control Sciences, Kitasato University, Tokyo, Japan | ²Department of Pediatrics, Sapporo Medical University School of Medicine, Sapporo, Japan | ³Department of Virology II, National Institute of Infectious Diseases, Tokyo, Japan | ⁴Department of Biochemistry and Cell Biology, National Institute of Infectious Diseases, Tokyo, Japan

Correspondence: Kei Haga (khaga@lisci.kitasato-u.ac.jp) | Kazuhiko Katayama (katayama@lisci.kitasato-u.ac.jp)

Received: 12 November 2024 | **Revised:** 27 January 2025 | **Accepted:** 9 February 2025

Transmitting Editor: Atsushi Miyawaki

Funding: This work was supported by Japan Society for the Promotion of Science, 21K08496, 24K11639. Japan Agency for Medical Research and Development, JP24fk0108667, JP24fk0108669.

Keywords: Caco-2 | cell culture | gastroenteritis | human sapovirus | neutralization

ABSTRACT

Human sapovirus (HuSaV), first identified in the 1970s, is a significant cause of acute gastroenteritis, particularly in young children. Despite its clinical significance, research on HuSaV has been limited due to the absence of a reliable cell culture system. In 2020, a breakthrough study reported that HuSaV GI.1 and GII.3 strains could be cultured and serially propagated using HuTu80 cells in the presence of bile acids. However, in 2024, a subsequent study reported that effective replication in HuTu80 cells requires specialized cells that have undergone over 100 passages. In this study, we sought to identify an alternative cell culture system for HuSaV. HuSaV GI.1 can replicate and be serially propagated using Caco-2 cells under bile acid supplementation. Importantly, the Caco-2 cells were freshly sourced from the American Type Culture Collection, ensuring reproducibility for laboratories worldwide. Furthermore, Caco-2MC cells were established via single-cell cloning from in-house Caco-2/Cas9 cells with 91.5% HuSaV-susceptible. HuSaV strains GI.1, GI.2, GI.3, GII.1, GII.3, and GV.1 were successfully propagated using Caco-2MC cells, with RNA copy numbers increasing up to 4.4 log₁₀-fold within 5 days post-infection. This efficient HuSaV cell culture system represents a significant advancement in HuSaV research.

1 | Introduction

Sapovirus (SaV), a member of the *Caliciviridae* family and *Sapovirus* genus, is a small, round, non-enveloped virus with a 30–38 nm diameter (Madeley 1979). The SaV genome comprises a positive-sense, ~7.1–7.7 kb single-stranded RNA divided into two open reading frames (ORFs). ORF1 encodes nonstructural proteins and the major capsid protein VP1, while ORF2 encodes the minor capsid protein VP2. SaV has been isolated from various species, including humans, pigs, dogs, sea lions,

and chimpanzees, and is currently classified into 19 genogroups (GI–GXIX) (Becker-Dreps et al. 2019). Human sapovirus (HuSaV) is categorized into 4 genogroups (GI, GII, GIV, and GV) and further divided into 19 genotypes, with GI.1 being the most frequently detected, followed by GI.2, GII.1, and GII.3 (Doan et al. 2023).

HuSaV was first identified in 1976 through electron microscopy of fecal samples from children with diarrhea in the UK (Madeley and Cosgrove 1976). Subsequently, a team from Sapporo

This is an open access article under the terms of the [Creative Commons Attribution-NonCommercial-NoDerivs](https://creativecommons.org/licenses/by-nc-nd/4.0/) License, which permits use and distribution in any medium, provided the original work is properly cited, the use is non-commercial and no modifications or adaptations are made.

© 2025 The Author(s). *Genes to Cells* published by Molecular Biology Society of Japan and John Wiley & Sons Australia, Ltd.

Medical University conducted detailed biological and genetic studies of a HuSaV-related acute gastroenteritis outbreak in an infant home in Sapporo, Japan (Chiba et al. 1979, 2000; Nakata et al. 2000; Numata et al. 1997). The strain collected in Sapporo in 1982 (Hu/SaV/Sapporo/1982/JPN) is now recognized as the *Sapovirus* genus prototype (Nakanishi et al. 2011). Together with human norovirus, HuSaV is among the leading causes of non-bacterial acute gastroenteritis worldwide. Although it affects all age groups, the disease burden is particularly high in children under 5 years of age (Becker-Dreps et al. 2019), with HuSaV isolated in 3%–17% of pediatric gastroenteritis cases in high- and low-income countries (Diez-Valcarce et al. 2018; Hassan et al. 2019; Sánchez et al. 2017). The severity of HuSaV gastroenteritis is generally milder than that caused by rotavirus or norovirus (Pang et al. 2000; Sakai et al. 2001), though hospitalizations may be required (Hansman et al. 2004; Medici et al. 2012; Park et al. 2015).

Since its discovery in the 1970s, research on HuSaV has been hindered by the absence of an efficient cell culture system or animal model for viral replication. However, in 2020, a breakthrough was made when a replication system for HuSaV GI.1 and GII.3 was established using the HuTu80 human duodenal cancer cell line in the presence of bile acids (Takagi et al. 2020). Nonetheless, a lack of HuSaV replication in HuTu80 cells was subsequently reported (Euller-Nicolas et al. 2023). Meanwhile, in 2024, Oka et al. reported that the successful replication of HuSaV requires specialized HuTu80 cells that have undergone over 100 passages, potentially accounting for the inability of other groups to replicate these experiments (Oka et al. 2024). Additionally, in 2023, HuSaV GI.1 and GI.2 were successfully cultured using human small intestinal enteroids, and HuSaV GI.1, GI.2, GII.1, GII.3, and GIV.1 were replicated in iPS-derived human intestinal epithelial cells (Euller-Nicolas et al. 2023; Matsumoto et al. 2023). However, these systems achieved lower replication levels than HuTu80 cells, and data demonstrating their ability to maintain continuous passaging are lacking. Hence, to drive further advances in HuSaV research, the establishment of a stable, reproducible culture system with efficient viral replication and the capability for continuous passage is essential.

In this study, we attempted to propagate HuSaV in various cell lines in search of new candidate cell lines that possess susceptibility to this virus. The RNA replication efficiencies and virus production capabilities of candidate cells were investigated.

2 | Results

2.1 | Screening of Cell Lines for Susceptibility to HuSaV Infection

To establish a stable and reproducible culture system for HuSaV, we screened cell lines susceptible to HuSaV infection. HuTu80, HEK293T, Caco-2, HCT15, and HCT116 cell lines were inoculated with a HuSaV GI.1 (AH20) positive stool suspension; the HuSaV RNA copy numbers in the culture supernatant at 0 or 1 day post-infection (dpi) and 7 dpi were compared. In 96-well plates, approximately 4×10^7 copies/well were applied to

HuTu80 and HEK293T cells, while 2×10^6 copies/well were used for Caco-2, HCT15, and HCT116 cells. In accordance with a previous study, 1000 μ M sodium glycocholate (GCA; Nacalai Tesque, Kyoto, Japan) was added in the infection assay (Takagi et al. 2020).

In HuTu80 and HEK293T cells, the HuSaV RNA copy number increased by 1.8 \log_{10} -fold (2.2×10^2 to 1.6×10^4 copies/ μ L) and 2.3 \log_{10} -fold (6.0×10^2 to 1.3×10^5 copies/ μ L), respectively, from 1 to 7 dpi (Figure 1A). In Caco-2 cells, HuSaV RNA was undetectable at 0 dpi but reached 1.7×10^4 copies/ μ L by 7 dpi, representing an increase of at least 3.2 \log_{10} (Figure 1B). In contrast, HCT15 cells exhibited low RNA levels at 7 dpi (9.4×10^1 copies/ μ L), and no detectable RNA was observed in HCT116 cells at 0 or 7 dpi. To estimate the proportion of infected cells, HuSaV VP1 protein was detected at 3 dpi by immunofluorescence staining, revealing only a few fluorescent cells in HuTu80 cells and slightly more in HEK293T cells expressing VP1 (Figure 1C). In contrast, a large fraction of Caco-2 cells exhibited VP1 expression, suggesting a higher proportion of susceptible cells.

Given the susceptibility of Caco-2 cells to HuSaV infection, we further tested Caco-2/Cas9 cells, previously shown to be highly susceptible to human astrovirus (HAstV) (Haga et al. 2024), and C2BBE1 cells, a clone derived from Caco-2 cells. The virus inoculum for these cells was the same as for Caco-2 cells ($\sim 2 \times 10^6$ copies/well). In Caco-2/Cas9 cells, HuSaV RNA levels rose drastically by 4.8 \log_{10} -fold to 9.1×10^5 copies/ μ L at 7 dpi, while C2BBE1 cells had undetectable RNA at 0 dpi and 6.3×10^1 copies/ μ L at 7 dpi (Figure 1B). Immunofluorescence staining of infected Caco-2/Cas9 cells revealed markedly more cells expressing VP1 (Figure 1C). Flow cytometry analysis at 4 dpi demonstrated that 19.1% of Caco-2 cells were positive for VP1 expression, while 38.8% of Caco-2/Cas9 cells were positive (Figure 1D). Hence, Caco-2-derived cells contained a larger susceptible population, potentially resulting in multiple infections.

2.2 | Serial Passage of HuSaV GI.1 Using Culture Supernatants

Serial passage experiments were conducted to verify the production of infectious progeny from each cell line. Culture supernatants from infected HuTu80, HEK293T, Caco-2, and Caco-2/Cas9 cells were collected at 7 dpi and inoculated into freshly prepared cultures of each respective cell line. In HuTu80 cells, the viral RNA copy number fell below the detection limit after the first passage (P + 1), indicating that further passaging was not possible (Figure 2A). In HEK293T cells, the RNA copy number increased by 1.8 \log_{10} -fold from 1 dpi to 7 dpi during the first passage (P + 1) but declined below the detection limit after the second passage (P + 2), preventing further propagation (Figure 2B). Conversely, Caco-2 and Caco-2/Cas9 cells supported stable increases in HuSaV RNA copy numbers from 0 dpi to 7 dpi across five passages (P + 5), with increases of 2.0–4.9 \log_{10} -fold in Caco-2 and 2.5 to 4.6 \log_{10} -fold in Caco-2/Cas9 cells, confirming successful serial passaging (Figure 2C,D). Thus, Caco-2 cells and Caco-2/Cas9 cells effectively produced infectious progeny viruses.

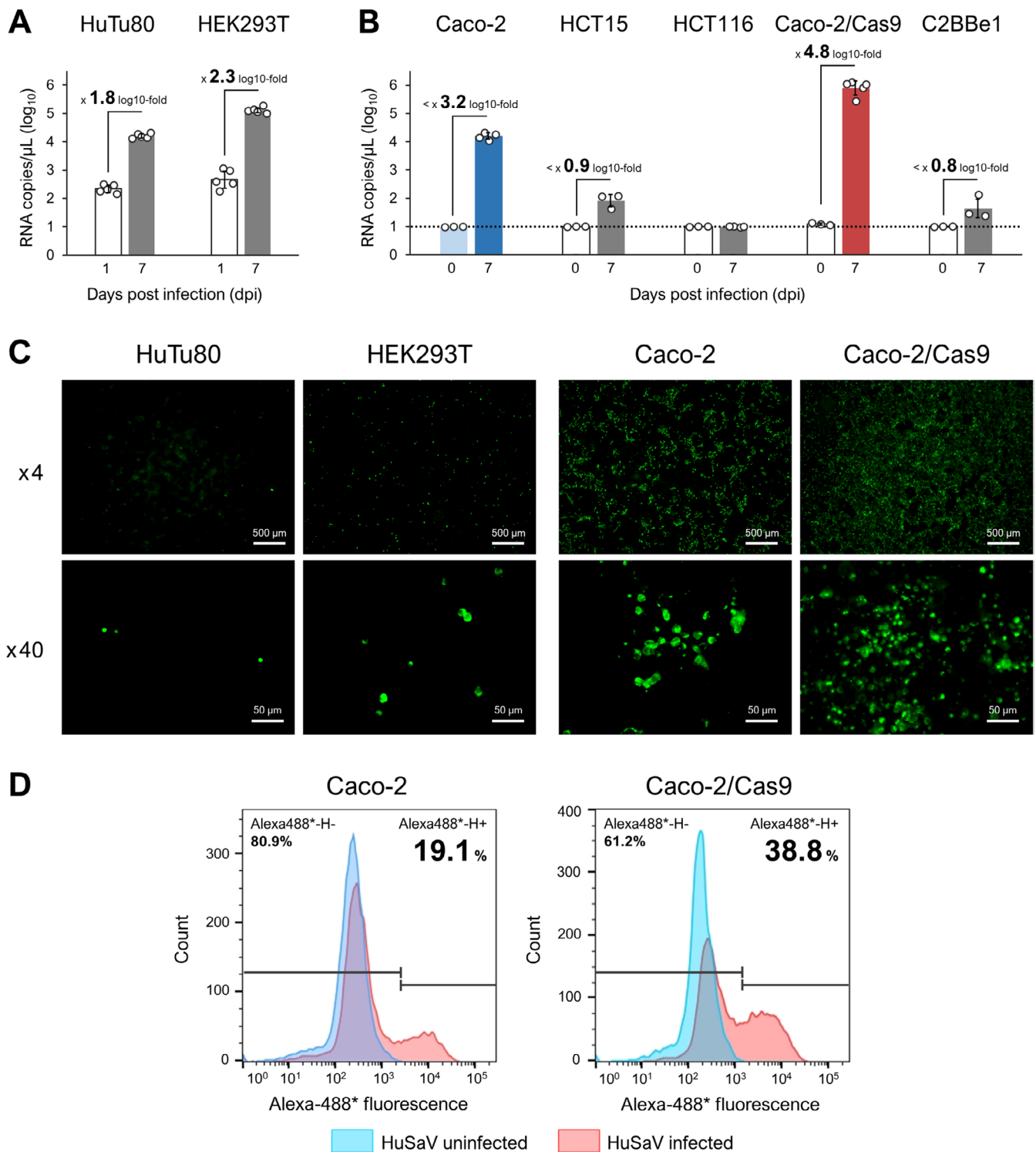


FIGURE 1 | Susceptibility of various cell lines to HuSaV infection. (A) Changes in HuSaV RNA copy numbers in the culture supernatants of HuTu80 and HEK293T cells following inoculation with a HuSaV GI.1 (AH20)-positive stool suspension ($\sim 4 \times 10^7$ copies/well in 96-well plates). Each dot represents individual data points; bars indicate the geometric mean value of the HuSaV RNA copy numbers; error bars denote the geometric standard deviation (SD). This experiment was performed once with five technical replicates. (B) Changes in HuSaV RNA copy numbers in the culture supernatants of Caco-2, HCT15, HCT116, Caco-2/Cas9, and C2BBE1 cells following inoculation with a HuSaV GI.1 (AH20)-positive stool suspension ($\sim 2 \times 10^6$ copies/well in 96-well plates). Each dot represents individual data points; bars indicate the geometric mean HuSaV RNA copy numbers; error bars denote the geometric SD. This experiment was performed once with five technical replicates. (C) Immunofluorescence staining of the viral protein VP1 in HuTu80, HEK293T, Caco-2, and Caco-2/Cas9 cells at 3 dpi with a HuSaV GI.1 (AH20)-positive stool suspension; upper panels: 4 \times objective lens, lower panels: 40 \times objective lens. (D) Flow cytometry analysis of Caco-2 and Caco-2/Cas9 cells infected with a HuSaV GI.1 (AH20)-positive stool suspension at 4 dpi. Blue: VP1-negative cells (uninfected), red: VP1-positive cells (infected).

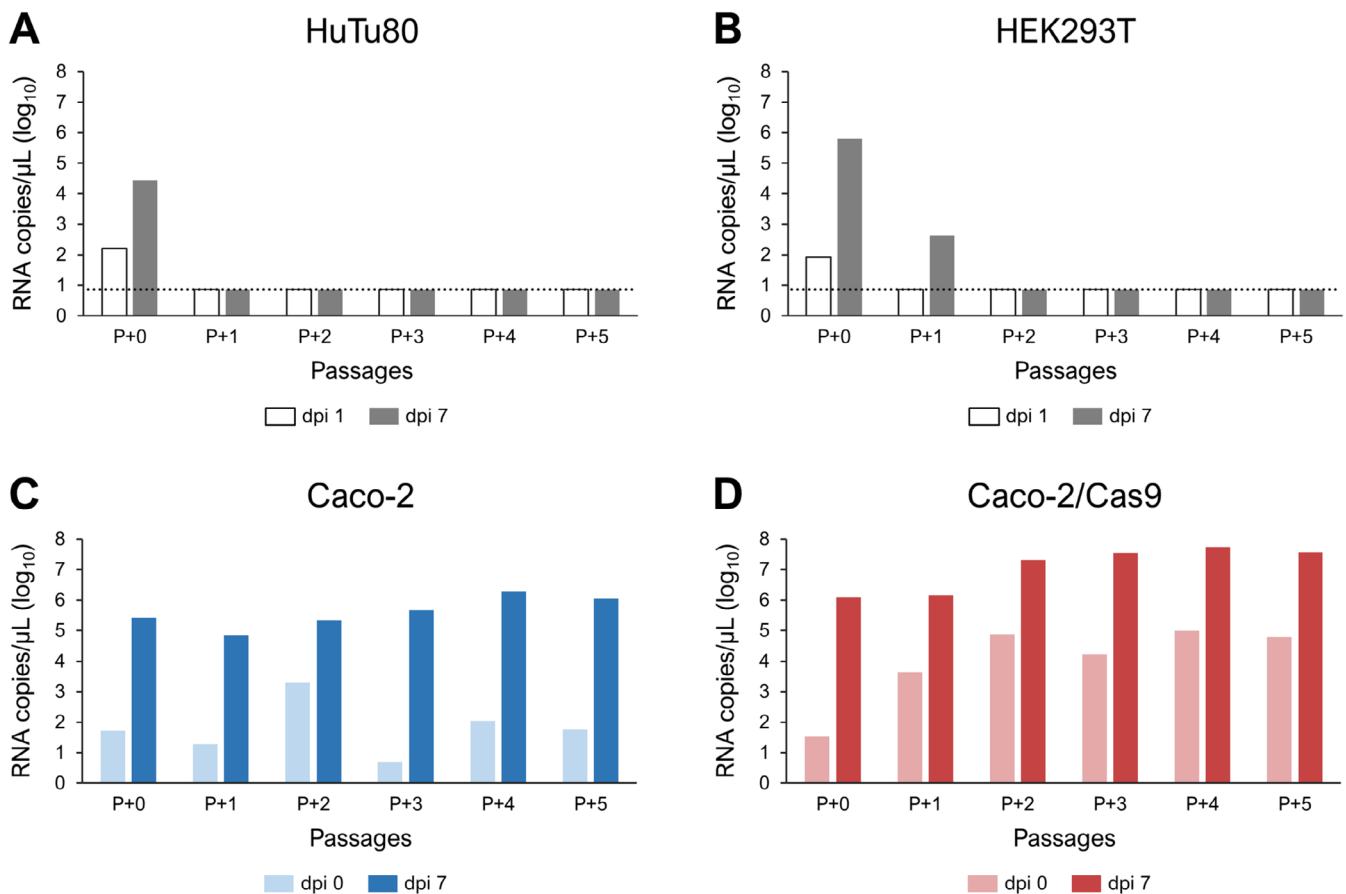


FIGURE 2 | Serial passage of HuSaV GI.1 in HuTu80, HEK293T, Caco-2, and Caco-2/Cas9 cells. HuSaV RNA copy numbers in the culture supernatants at 0 or 1 dpi (immediately after medium replacement) and 7 dpi for each passage, up to P + 5, in (A) HuTu80, (B) HEK293T, (C) Caco-2, and (D) Caco-2/Cas9 cells.

2.3 | Requirement of Bile Acids for HuSaV Replication in Caco-2/Cas9 Cells

Previous studies have indicated that bile acids are essential for HuSaV replication using HuTu80 cells (Takagi et al. 2020). Hence, the bile acid requirement for HuSaV replication in Caco-2/Cas9 cells was evaluated. To this end, the HuSaV RNA copy number changes from 0 to 7 dpi were comparatively examined with different bile components (1000 μ M GCA, 500 μ M sodium glycochenodeoxycholate [GCDCA; Sigma, MAs, USA], or 0.5% porcine bile [Sigma]) in the culture media.

GCA, GCDCA, and porcine bile resulted in 4.0, 3.7, and 3.3 \log_{10} -fold increases in HuSaV RNA, respectively, from 0 to 7 dpi. GCA induced the highest replication efficiency (Figure 3). Without bile components, the RNA increase was limited to 1.0 \log_{10} -fold. These findings indicate that adding bile acids is crucial for efficient HuSaV replication in Caco-2/Cas9 cells. Based on these results, 1000 μ M GCA was selected for use in subsequent HuSaV infection experiments.

2.4 | Production and Release of Viral Particles in Caco-2/Cas9 Cells

To assess the production and release of viral particles from HuSaV GI.1-infected Caco-2/Cas9 cells, viral particles were purified from

both the culture supernatant and cell lysate via CsCl density gradient ultracentrifugation. After fractionation based on buoyant density, viral RNA copy numbers in each of the 12 fractions were quantified by quantitative reverse transcription polymerase chain reaction (RT-qPCR). In the culture supernatant, fractions 1–4 (1.299–1.325 g/cm³) exhibited higher RNA copy numbers, while in the cell lysate, fractions 8–11 (1.367–1.420 g/cm³) showed higher RNA copy numbers (Figure 4A).

Electron microscopy was performed on the fractions with the highest HuSaV RNA copy numbers: fractions 1, 2, 9, and 10 from the supernatant, and fractions 9, 10, and 11 from the lysate (Figure 4A). In the culture supernatant, viral particles were detected only in fraction 1 (1.299 g/cm³), while no particles were detected in fractions 2, 9, and 10 (Figure 4B). In contrast, numerous viral particles were observed in the cell lysate, particularly in fractions 10 and 11 (1.399–1.420 g/cm³), with aggregated particles. Western blot analysis further confirmed the presence of VP1 protein in these viral particles-containing fractions (Figure 4C).

To further assess infectivity, low-density fraction 1 (1.299 g/cm³) and high-density fraction 10 (1.399 g/cm³) from the culture supernatant and cell lysate were re-inoculated into Caco-2/Cas9 cells. Immunofluorescence for VP1 at 3 dpi revealed fluorescence in cells inoculated with both the low-density fraction 1 (from the culture supernatant and cell lysate) and high-density fraction 10 (from the cell lysate) (Figure 4D). Notably, more

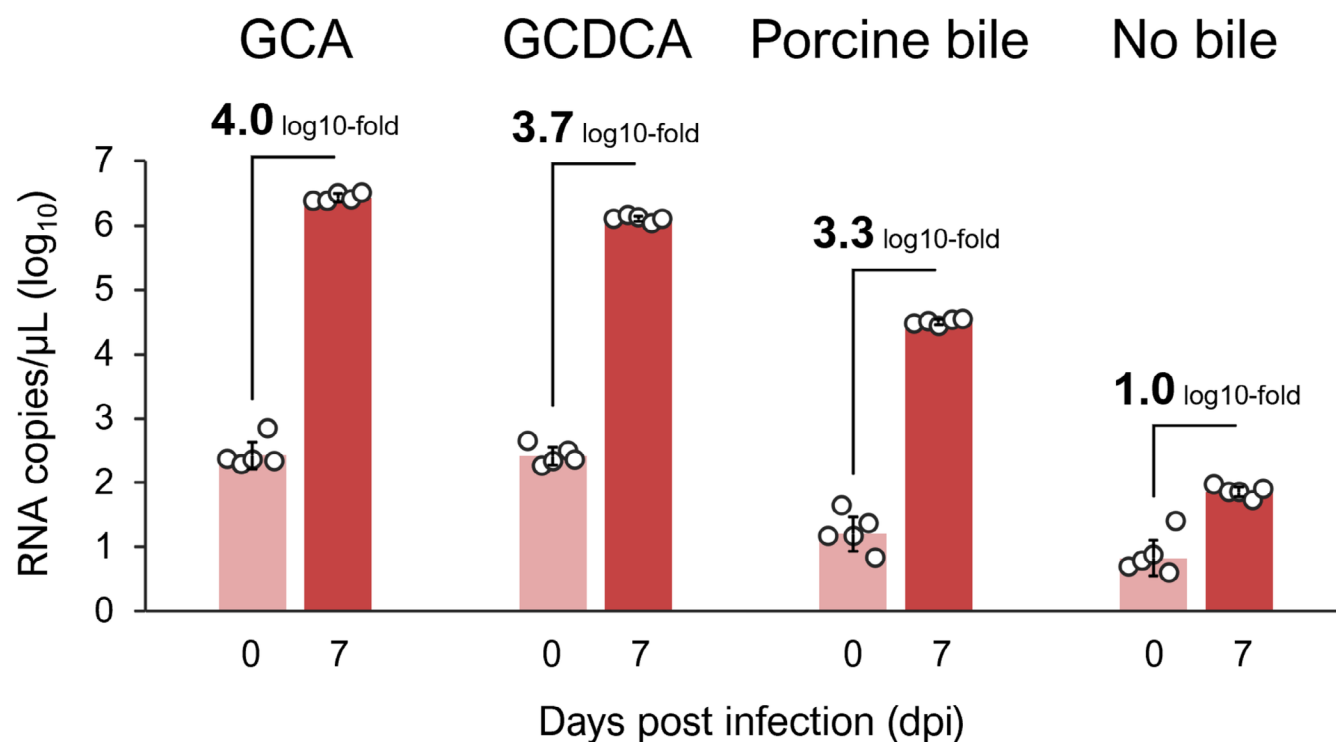


FIGURE 3 | Effect of different bile acids on HuSaV replication efficiency in Caco-2/Cas9 cells. Caco-2/Cas9 cells were inoculated with HuSaV GI.1 (AH20)-positive stool suspension (approximately 4×10^7 copies/well in 96-well plates) and incubated at 37°C for 3 h. HuSaV RNA copy numbers in the culture supernatants were measured at 0 dpi (immediately after medium replacement) and 7 dpi with different bile acids in the culture media. Each dot represents individual data points; bars indicate the geometric mean HuSaV RNA copy numbers; error bars represent the geometric SD. This experiment was performed once with five technical replicates. GCA, Sodium glycocholate; GCDCA, sodium glycochenodeoxycholate.

fluorescent cells were detected following inoculation with the cell lysate fractions compared to the supernatant fractions.

These results demonstrate that infectious HuSaV particles were successfully produced and released from infected Caco-2/Cas9 cells. Furthermore, a higher proportion of infectious viral particles is retained within the cells compared to the culture supernatant.

2.5 | Cloning of Caco-2MC Cells With High HuSaV Susceptibility

The proportion of infected Caco-2/Cas9 cells was higher than that of the parental Caco-2 cells (38.8% vs. 19.1%; Figure 1D). Caco-2/Cas9 cells were created by introducing the Cas9 gene into Caco-2 cells, and six of 17 clones with high HAsV type 4 susceptibility were selected and combined (Haga et al. 2024). We aimed to create a cell line with increased susceptibility to HuSaV by performing single-cell cloning from the Caco-2/Cas9 population. To this end, Caco-2/Cas9 cells were diluted to a density of 0.5 cells/well in a 96-well plate and cultured to confluence. Sixteen clones, designated A through P (Caco-2A–P), were generated and subsequently infected with HuSaV GI.1. Immunofluorescence staining at 4 dpi revealed that clone M (Caco-2M) exhibited the highest proportion of infected cells, while clone P (Caco-2P) showed minimal VP1 fluorescence (Figures 5A and S1).

To further increase the proportion of HuSaV-susceptible cells, an additional round of single-cell cloning was performed using Caco-2M cells. Six clones were generated using the same

dilution method (Caco-2MA, MC, ME, MH, MN, and MP), all reaching confluence. These clones were then infected with HuSaV GI.1; flow cytometry analysis at 4 dpi revealed that clone MC (Caco-2MC) and clone ME (Caco-2ME) had the highest susceptibility rate, with 91.5% of cells infected, compared to 79.9% in the parental Caco-2M cells (Figures 5B and S2). Thus, Caco-2MC cells were selected for subsequent infection experiments. Immunofluorescence staining of HuSaV-infected Caco-2MC cells at 4 dpi revealed that VP1 was distributed throughout the cytoplasm in a granular pattern, with prominent localization around the nucleus (Figure 5C). Furthermore, double staining for NS3 or NS7 and VP1 in HuSaV-infected Caco-2MC cells showed that cells positive for VP1 also exhibited fluorescence signals for NS3 and NS7 (Figure S3).

Caco-2P cells, with minimal VP1 fluorescence, were also subjected to single-cell cloning, generating clones PA through PT (Caco-2PA–PT). Infection with HuSaV GI.1 resulted in only 0.05% of cells in clone PG (Caco-2PG) exhibiting VP1 fluorescence at 4 dpi (Figures 5D and S4).

2.6 | Dynamics of HuSaV RNA Copy Numbers and Infectivity Following HuSaV Infection

Considering that the progeny virus was more abundant in cells than in the culture supernatant, to further optimize the HuSaV culture system, the dynamics of HuSaV RNA copy numbers and infectivity were examined in the culture supernatant and cells of the Caco-2MC line. RT-qPCR and median tissue culture

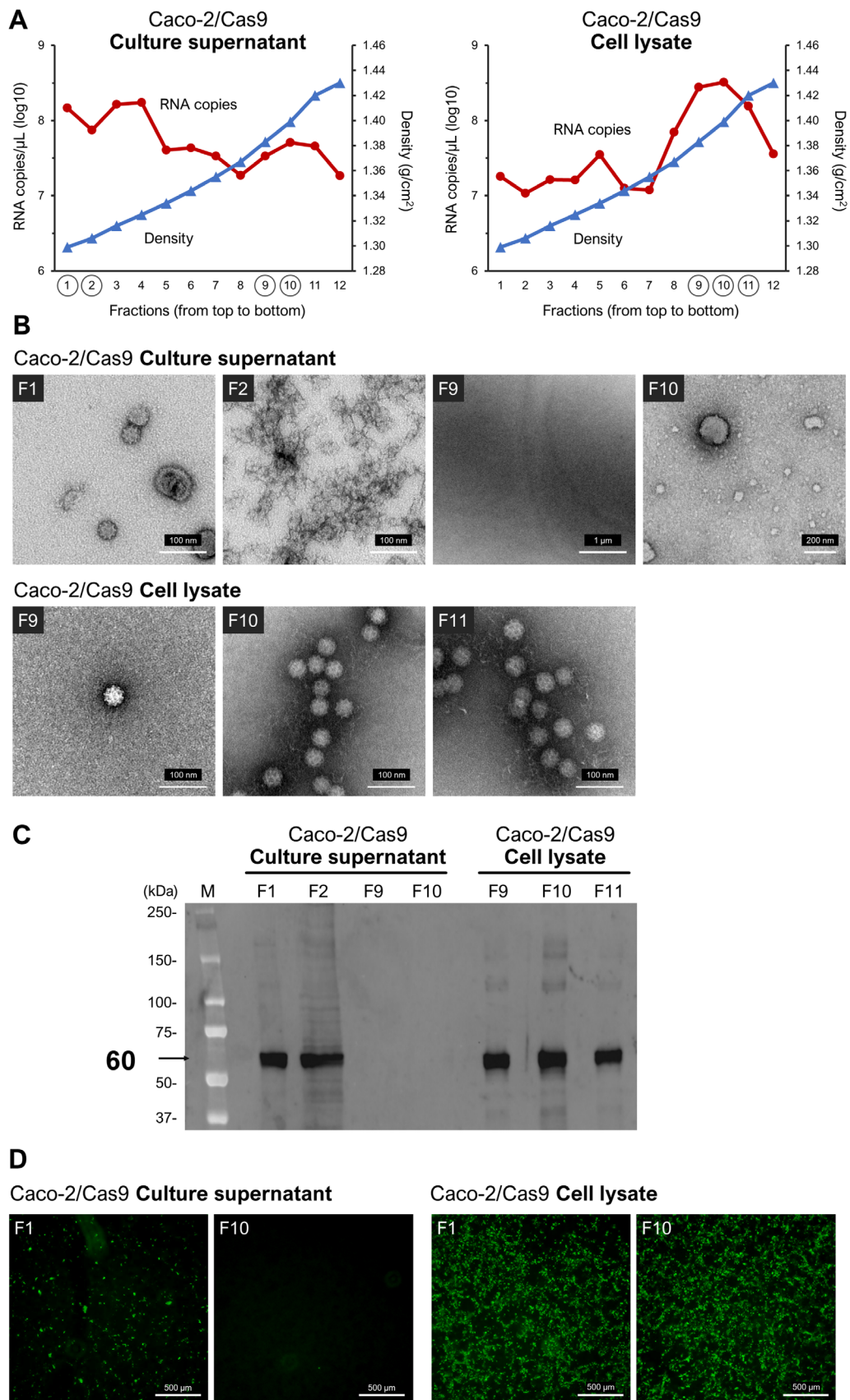


FIGURE 4 | Legend on next page.

FIGURE 4 | Purification of HuSaV GI.1 from infected Caco-2/Cas9 cells with CsCl density-gradient ultracentrifugation. (A) HuSaV RNA copy numbers and density profiles across fractions from culture supernatants and cell lysates. Fractions marked with circles on the x-axis were selected for subsequent electron microscopy western blotting analyses. (B) Electron microscopy of fractions 1, 2, 9, and 10 from the culture supernatants and fractions 9, 10, and 11 from the cell lysates. (C) Western blotting detection of the capsid protein VP1. The 60kDa protein band, indicated by an arrow, corresponds to VP1. (D) Immunofluorescence staining for VP1 in Caco-2/Cas9 cells at 3 dpi following re-infection with fractions 1 and 10 from the culture supernatants and cell lysates.

infectious dose (TCID₅₀) assays were used to compare these parameters. Caco-2MC cells were infected with HuSaV GI.1 at a multiplicity of infection (MOI) of 0.01. To compare viral quantities and infectivity between the cell lysate and culture supernatant, infected cells were lysed using the same volume of distilled water (DW) as the culture supernatant to release intracellular viruses.

The number of HuSaV RNA copies in the culture supernatant increased steadily from 2.0×10^2 copies/ μ L at 0 dpi to 4.2×10^5 copies/ μ L at 7 dpi, representing a 3.6 log₁₀-fold increase (Figure 6A). In the cell lysate, HuSaV RNA copy numbers increased from 6.9×10^3 copies/ μ L at 0 dpi to 5.4×10^7 copies/ μ L at 5 dpi, a 3.9 log₁₀-fold increase, and remained stable through 7 dpi (6 dpi: 2.9×10^7 copies/ μ L, 7 dpi: 8.5×10^7 copies/ μ L).

The TCID₅₀ assays revealed gradually increasing infectivity titers in the culture supernatant and cell lysate from 1 dpi, peaking at 5 dpi, and slightly decreasing by 6 and 7 dpi (Figure 6B). By 5 dpi, the infectivity titer in the cell lysate was 6.4×10^7 TCID₅₀/mL, 640 times higher than in the culture supernatant (1.0×10^5 TCID₅₀/mL). These findings suggest that the infectious viruses were more abundant in cells; thus, extracting viruses from cells would be a more efficient approach for HuSaV culture.

Caco-2MC cells infected with HuSaV GI.1 began to exhibit cytopathic effects (CPE) around 3 dpi, with some cells exhibiting detachment by 6 and 7 dpi (Figure 6C). In contrast, mock-infected Caco-2MC cells showed no obvious damage by 7 dpi.

2.7 | Requirement of Bile Acids for HuSaV Replication in Caco-2MC Cells

In the previous experiment, efficient HuSaV GI.1 replication in Caco-2/Cas9 cells was achieved by adding 1000 μ M GCA (Figure 3). To evaluate the bile acid requirement in Caco-2MC cells, a similar experiment was conducted with 1000 μ M GCA, 500 μ M GCDCA, 0.5% porcine bile, or no bile components added to the culture media. Changes in RNA copy numbers in cell lysates were assessed from 0 to 5 dpi.

GCA, GCDCA, and porcine bile resulted in 2.5, 2.4, and 1.9 log₁₀-fold increases in HuSaV RNA, respectively, while the increase without bile components was limited to 0.4 log₁₀-fold (Figure 7). These results confirm that, similar to that in Caco-2/Cas9 cells, 1000 μ M GCA promotes efficient HuSaV replication in Caco-2MC cells.

2.8 | Serial Passaging of Multiple HuSaV Genotypes Using Cell Lysate

Multiple HuSaV genotypes were serially passaged by infecting highly susceptible Caco-2MC cells with viruses from high-titer cell lysates. Stool suspensions positive for HuSaV GI.1 (M13-18, Ni17-9, and E22-22), GI.2 (M13-6), GI.3 (I21-042), GII.1 (TKC19-5 and TKC19-10), GII.3 (I22-124), GIV.1 (IB-02 and KA-31), and GV.1 (EH-40 and IB-24) were used to infect Caco-2MC cells. The cell lysates obtained at 5 dpi were subsequently used to infect a fresh layer of confluent Caco-2MC cells. In all 10 samples, excluding the two GIV.1 samples, a significant increase in HuSaV RNA copy numbers was observed from 0 to 5 dpi (increases ranging from 1.7- to 4.4-log₁₀ fold), that is, the second passage (P + 2), indicating successful passaging (Figure 8). In contrast, both GIV.1 samples showed no increase in RNA copy numbers at 5 dpi following inoculation with stool suspensions, preventing further passage. Additional experiments using four other GIV.1 samples (KU-18, OS-283, OS-286, and OS-287) similarly showed no replication (Figure S5). These results suggest that Caco-2MC cells are useful for amplifying HuSaV genogroups GI, GII, and GV in vitro, excluding GIV.

2.9 | HuSaV GI.1 Neutralization Assay Using Caco-2MC Cells

To evaluate whether a neutralization assay for HuSaV GI.1 could be conducted using Caco-2MC cells, HuSaV GI.1, adjusted to 50 TCID₅₀, was mixed in equal volumes with 5-fold serial dilutions of anti-rabbit HuSaV GI.1 VLP hyperimmune serum or nonimmunized rabbit serum. The mixture was inoculated into Caco-2MC cells seeded in a 96-well plate. At 5 dpi, the HuSaV RNA copy numbers were quantified in the culture supernatant and cell lysate to assess the neutralization efficacy.

In wells with anti-rabbit GI.1 VLP serum diluted between 1:5⁵ and 1:5⁷, mean RNA copy numbers ranged from 6.0×10^3 to 1.1×10^4 copies/ μ L in the cell lysate and 1.8 to 3.8×10^3 copies/ μ L in the culture supernatant (Figures 9A and S6A). However, when the anti-rabbit GI.1 VLP serum was diluted beyond 1:5⁸, RNA copy numbers increased; at dilutions of 1:5¹⁰ to 1:5¹², mean RNA copy numbers in the cell lysate ($2.3\text{--}7.1 \times 10^6$ copies/ μ L) and culture supernatant ($3.1\text{--}9.7 \times 10^5$ copies/ μ L) were comparable to those in wells with non-immunized rabbit serum (Figures 9 and S6). These findings demonstrate that HuSaV GI.1 neutralization can be achieved using anti-rabbit HuSaV GI.1 VLP serum in Caco-2MC cells.

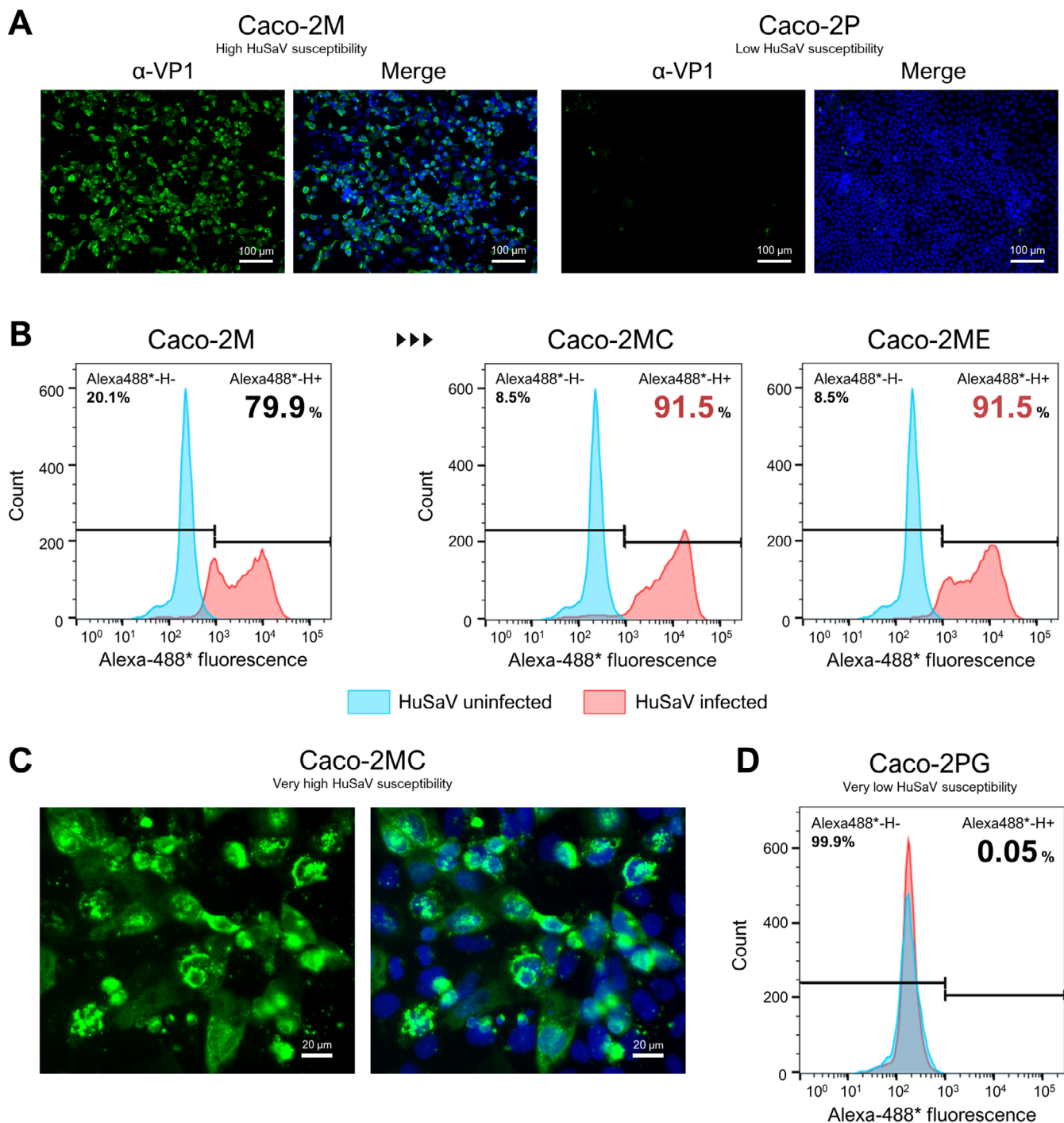


FIGURE 5 | Immunofluorescence and flow cytometry analysis of highly HuSaV-susceptible Caco-2MC cells. (A) Immunofluorescence staining at 4 dpi with HuSaV GI.1 (AH20) on cloned cells derived from Caco-2/Cas9 cells; (left) clone M (Caco-2M), (right) clone P (Caco-2P); blue: Nuclei (Hoechst). (B) Flow cytometry at 4 dpi following infection with HuSaV GI.1 (AH20) in Caco-2M, Caco-2MC, and Caco-2ME cells; blue: VP1-negative cells (uninfected), red: VP1-positive cells (infected). (C) Immunofluorescence staining of Caco-2MC cells at 4 dpi following infection with HuSaV GI.1 (AH20). (D) Flow cytometry at 4 dpi following infection with HuSaV GI.1 (AH20) in Caco-2PG cells.

3 | Discussion

In this study, the human colorectal adenocarcinoma cell line Caco-2 was found to be susceptible to HuSaV GI.1 infection in the presence of bile acids. Moreover, HuSaV was successfully serially passaged using the culture supernatant from infected cells. Since the Caco-2 cells used in these experiments were recently acquired from the American Type Culture Collection

(ATCC), the results should be reproducible in various research settings globally. In contrast, infection of HuTu80 cells with HuSaV GI.1 was unsuccessful, although this cell line has been previously reported to support HuSaV GI.1 replication (Takagi et al. 2020). As suggested by Oka et al., successful replication in HuTu80 cells may require highly passaged cells; newly obtained HuTu80 cells from ATCC may not support HuSaV replication (Oka et al. 2024). Additionally, while HEK293T cells

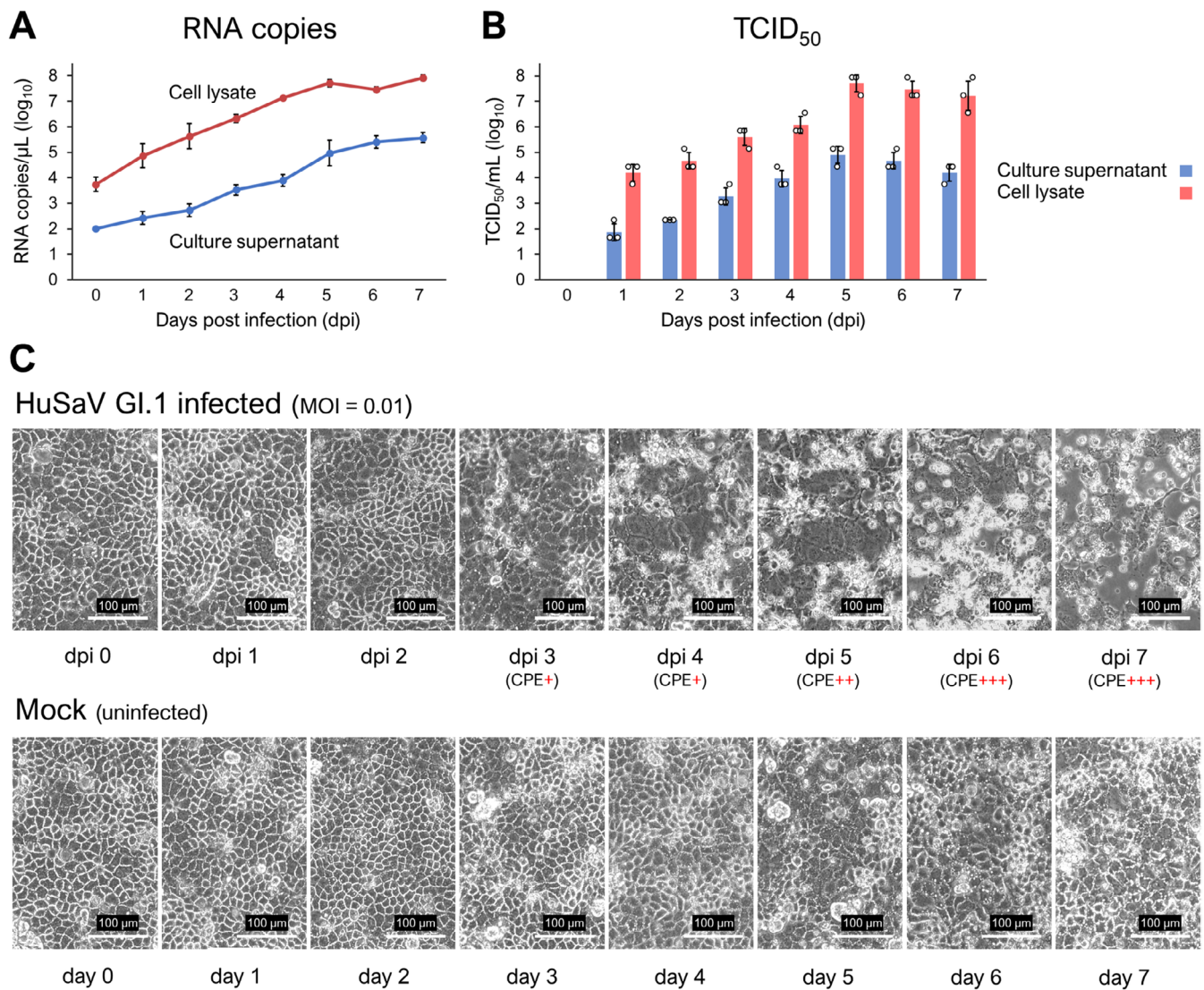


FIGURE 6 | Time-course analysis of RNA copy numbers and TCID₅₀ in HuSaV-infected Caco-2MC cells. (A) Time-course changes in RNA copy numbers in culture supernatants and cell lysates from 0 to 7 dpi. Circular dots indicate the geometric mean values of the HuSaV RNA copy numbers, and error bars represent geometric SD. This experiment was performed once with three technical replicates. (B) Time-course changes in TCID₅₀ values in supernatants and cell lysates from 0 to 7 dpi. Each dot represents individual data points; bars indicate the geometric mean TCID₅₀ values; error bars represent geometric SD. This experiment was performed once with three technical replicates. (C) Phase-contrast microscopy images of Caco-2MC cells from 0 to 7 dpi; (top) HuSaV GI.1-infected Caco-2MC cells, (bottom) uninfected control cells.

supported HuSaV replication, they could not sustain serial passaging.

Several studies suggest that HuSaV primarily infects the small intestine. For instance, Euller-Nicolas et al. reported that HuSaV GI.1 and GI.2 replicate exclusively in the small intestine, not in the colon, as assessed by using human intestinal enteroids (Euller-Nicolas et al. 2023). Moreover, Guo et al. detected porcine sapovirus, morphologically and genetically similar to HuSaV, in cells of the small intestine with corresponding villi shortening and blunting; no such findings were observed in the colon (Guo et al. 2001). Although Caco-2 cells originate from human colon adenocarcinoma (Fogh et al. 1977), they differentiate into small intestine-like cells upon reaching confluence (Engle et al. 1998), likely accounting for their susceptibility to HuSaV infection.

Notably, our results contrast those of Oka et al., who reported in 2018 that they could not replicate HuSaV in Caco-2 cells in the presence of GCDCA (Oka et al. 2018). However, they tested only one HuSaV GI.2 sample, which may have created a suboptimal condition for infection. Indeed, Caco-2 cells are heterogeneous, and subpopulations with varying characteristics can emerge depending on the culture conditions (Lea 2015). Thus, during the passaging process, the proportion of non-susceptible cells may have increased, hindering their successful replication.

Moreover, Caco-2/Cas9 cells, previously established in our laboratory and deemed highly susceptible to HAdV (Haga et al. 2024), exhibited greater susceptibility to HuSaV than Caco-2 cells. This increased susceptibility could be due to a higher proportion of HuSaV-susceptible subpopulations in the

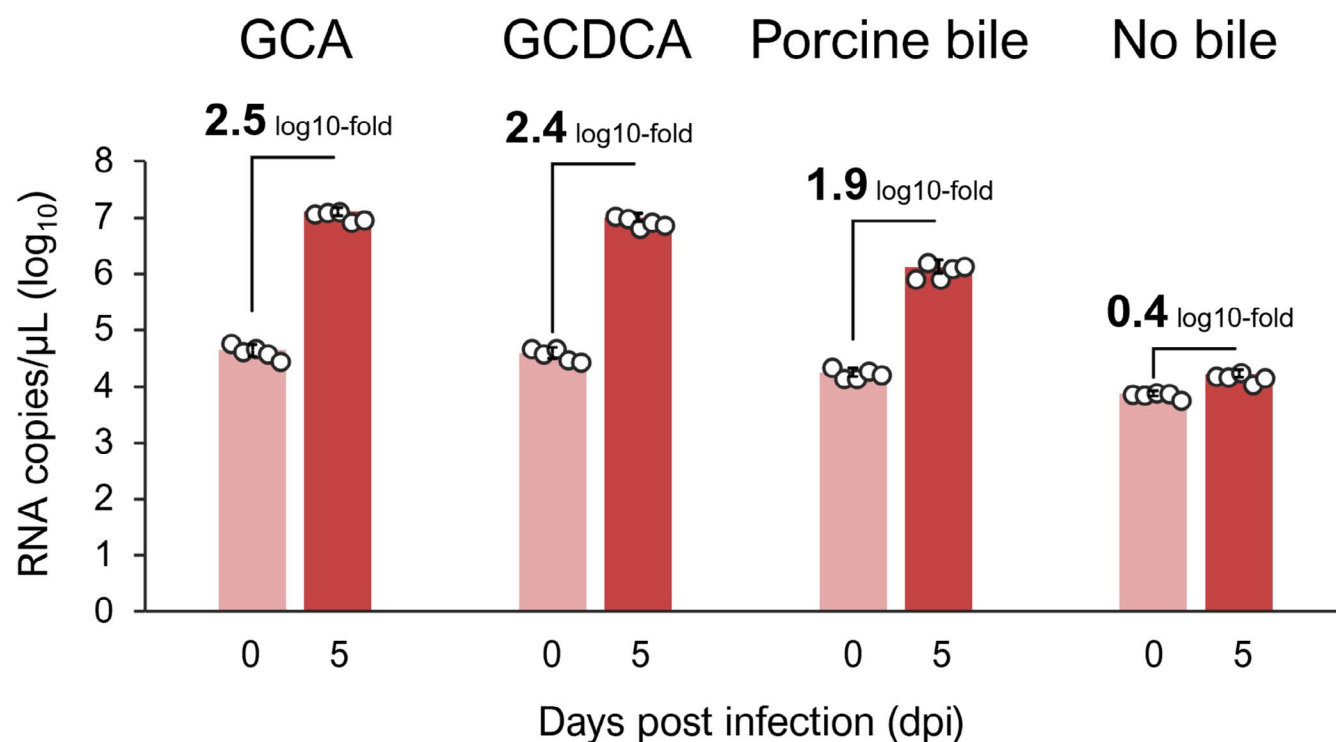


FIGURE 7 | Effect of different bile acids on HuSaV replication efficiency in Caco-2MC cells. Caco-2MC cells were inoculated with HuSaV GI.1 (M13-18) stock at an MOI of 0.01 and incubated at 37°C for 3 h. HuSaV RNA copy numbers in the cell lysates were measured at 0 dpi (after 3 h incubation) and 5 dpi with different bile acids in the culture media. Each dot represents individual data points; bars indicate the geometric mean HuSaV RNA copy numbers; error bars represent the geometric SD. This experiment was performed three times with five technical replicates. GCA, sodium glycocholate; GCDCA, sodium glychenodeoxycholate.

Caco-2/Cas9 cells. Furthermore, through repeated cloning of the Caco-2/Cas9 cells, the Caco-2MC cell line was established, 91.5% of which were susceptible to HuSaV infection. Using Caco-2MC cells, HuSaV GI.1, GI.2, GI.3, GII.1, GII.3, and GV.1 were successfully serially passaged. This represents a significant advancement in HuSaV research by establishing a stable cell culture system capable of supporting serial passaging, providing an alternative to HuTu80 cells.

However, HuSaV GIV.1 could not replicate in Caco-2MC cells. Similarly, previous studies using HuTu80 cells or an intestinal enteroid system failed to observe GIV.1 replication (Euller-Nicolas et al. 2023; Oka et al. 2024). Although replication has been reported using an iPS-derived intestinal enteroid system, the RNA copy number increase was limited to 13.9-fold, with no evidence of successful serial passaging (Matsumoto et al. 2023). The reason why GIV.1 fails to replicate in Caco-2MC cells, despite their human gastrointestinal origin, remains unclear and warrants further investigation.

Electron microscopy revealed that HuSaV particles were more abundant intracellularly than in the culture supernatant. Time-course analysis of HuSaV RNA copy numbers and TCID₅₀ in the culture supernatant and cell lysates further suggested that higher titers of infectious HuSaV exist intracellularly. While HuSaV GI.1 can be passaged using the culture supernatant, it is preferable to isolate viruses from cell lysates for higher titer passaging. Furthermore, HuSaV infectivity tends to decrease post-infection, a trend also reported in other viruses, such as severe acute respiratory syndrome coronavirus 2 (SARS-CoV-2) (Lina

et al. 2019; Mautner et al. 2022). As a useful reference for future studies, peak infectivity was observed at 5 dpi with an MOI of 0.01 in the current study.

CsCl density-gradient ultracentrifugation of HuSaV-infected cell lysates revealed viral particles predominantly at 1.383–1.420 g/cm³, consistent with previous reports (Suzuki et al. 1979; Terashima et al. 1983). Interestingly, infectivity was also detected in the low-density fractions F1 and F2, with a density of 1.299–1.306 g/cm³. In a study where HuSaV GII.3 was generated using a reverse genetics system in HuTu80 cells, complete viral particles were predominantly observed at 1.350 g/cm³, while the 1.286 g/cm³ fraction contained numerous empty particles (Li et al. 2022). The detection of infectious particles in the low-density F1 and F2 fractions is surprising, as this density corresponds to the empty particles reported in previous studies. This contradiction remains unexplained. Additionally, no viral particles were detected in the high-density fractions of the culture supernatant. HuSaV may be formed as high-density viral particles within Caco-2/Cas9 cells but undergoes processing that releases lower-density particles. Further investigation is necessary to clarify these findings.

Immunostaining of HuSaV GI.1-infected Caco-2MC cells revealed VP1 distribution throughout the cytoplasm and localization within granules around the nucleus. Similar observations have been reported for murine norovirus (MuNoV) in RAW264.7 cells, with replication intermediates (dsRNA) and non-structural proteins localized around the nucleus (Hyde et al. 2009). Immunoelectron microscopy has shown that MuNoV replication complexes are associated with virus-induced membrane

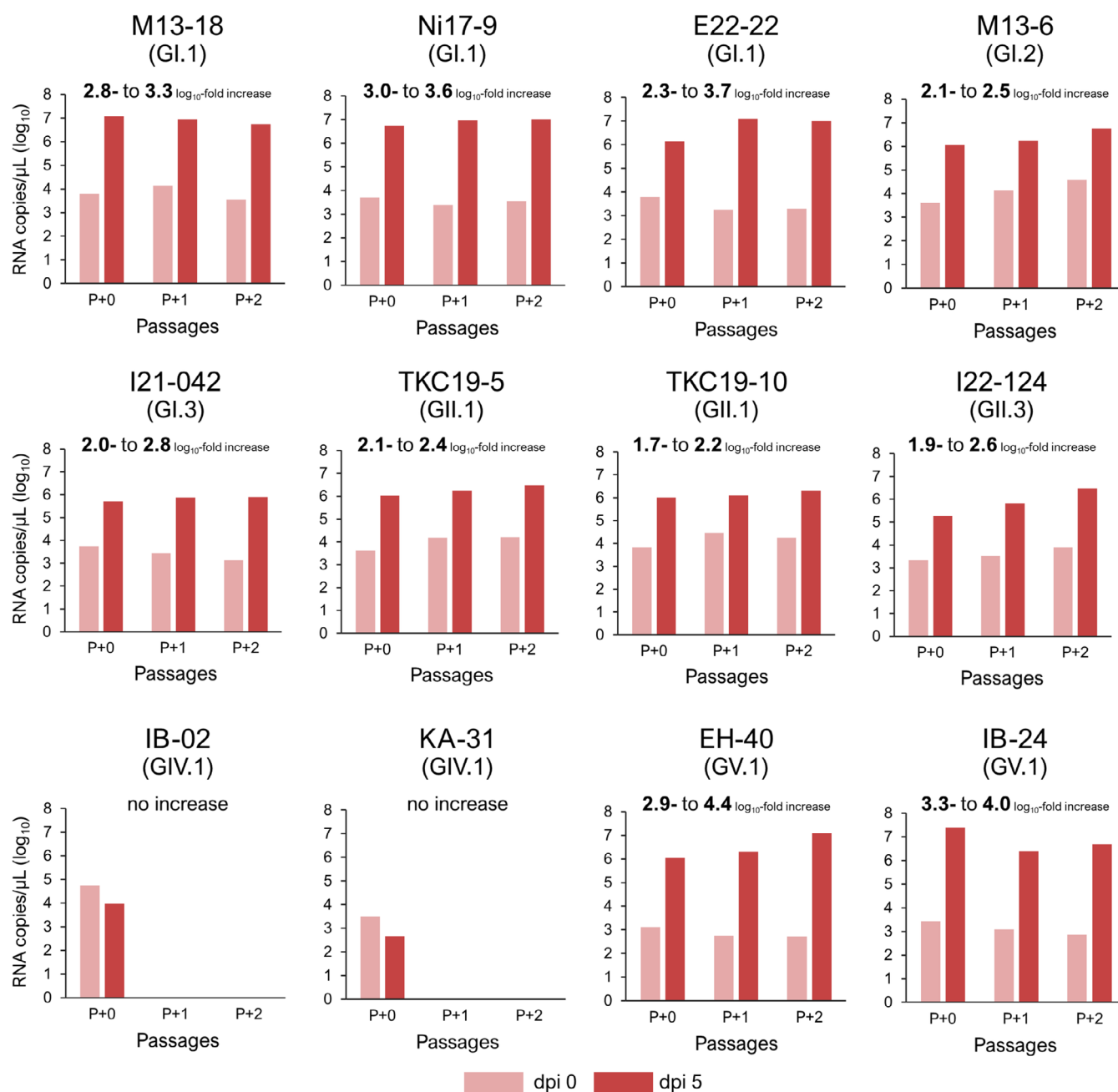


FIGURE 8 | Serial passaging of multiple HuSaV genotypes in Caco-2MC cells. The bar graphs show the HuSaV RNA copy numbers in the cell lysates at 0 and 5 dpi for each passage.

vesicles near the nucleus (Hyde et al. 2009), suggesting a similar replication mechanism for HuSaV. Future studies should utilize antibodies targeting HuSaV non-structural proteins, as well as electron microscopy and immunoelectron microscopy of HuSaV-infected cells, to further elucidate the HuSaV replication cycle.

In this study, HuSaV GI.1 infection was effectively neutralized in Caco-2MC cells using rabbit antiserum against HuSaV GI.1 VLP. The neutralization assay system in Caco-2MC cells allows for evaluation based on RNA copy numbers from the culture supernatant and cell lysates at 5 dpi. While additional studies are needed to determine whether the antiserum against HuSaV GI.1 VLP cross-reacts with other genotypes, our results show that Caco-2MC cells can be used for neutralization assays.

Accordingly, this system is a tool for evaluating vaccine efficacy and conducting seroepidemiological studies.

Although the results presented in this study align with previous findings and provide valuable insights, certain limitations should be acknowledged. Specifically, not all experiments were conducted with multiple independent replicates, which may influence the reproducibility of some data.

In conclusion, we successfully established a Caco-2-based cell line that is highly susceptible to HuSaV, validated for multiple genotypes, including GI.1, GI.2, GI.3, GII.1, GII.3, and GV.1. As a valuable alternative to HuTu80 cells, this cell line provides a robust platform for HuSaV research, including the development

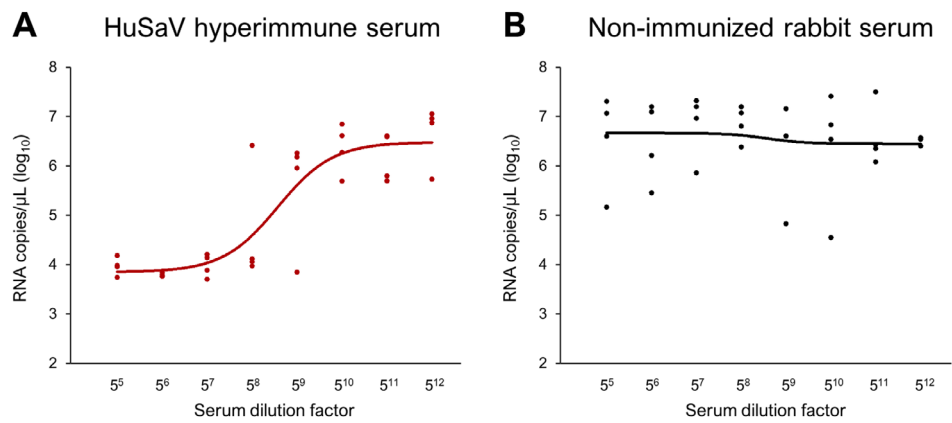


FIGURE 9 | HuSaV neutralization assay using Caco-2MC cells. HuSaV RNA copy numbers in the cell lysate at 5 dpi. Panel (A) shows results using anti-rabbit HuSaV VLP GI.1 VP1 hyperimmune serum, while panel (B) shows results with non-immunized rabbit serum. Each dot represents an individual data point, and curves were fitted using nonlinear regression in GraphPad Prism 8. This experiment was performed once with four technical replicates.

TABLE 1 | HuSaV-positive stool samples used in this study.

HuSaV genotype	Strain	Patient	Stool sample collection date	Viral RNA copy number (copies/μL of 10% stool suspension)	Accession number
GI.1	AH20	3-year-old	February 2020	4.0×10^7	LC671561
	M13-18	8-month-old	November 2013	1.4×10^7	LC842317
	Ni17-9	3-year-old	March 2017	2.7×10^6	LC842321
	E22-22	10-month-old	May 2022	5.4×10^6	LC842313
GI.2	M13-6	1-year-old	June 2013	6.1×10^6	LC842322
GI.3	I21-042	Pre-schooler	June 2021	2.8×10^6	LC842323
GII.1	TKC19-5	1-year-old	November 2019	1.8×10^7	LC842325
	TKC19-10	1-year-old	November 2019	2.4×10^7	LC842324
GII.3	I22-124	Pre-schooler	January 2023	1.0×10^7	LC842327
GIV.1	IB-02	Not available	2008	1.4×10^7	LC504424
	KA-31	Not available	2013	5.3×10^5	LC504425
GV.1	EH-40	Not available	2014	6.7×10^5	LC504434
	IB-24	Not available	2014	2.2×10^6	LC504440

of vaccines and antiviral drugs, receptor discovery, and epidemiological studies.

4 | Experimental Procedures

4.1 | Stool Samples

The stool samples used in this study were collected from patients in Japan, as outlined in Table 1. To prepare a 10% (w/v) stool suspension, an appropriate amount of stool was weighed and suspended in Dulbecco's phosphate-buffered saline without Mg^{2+} and Ca^{2+} (D-PBS (–); Nacalai Tesque). The stool suspension was thoroughly vortexed and centrifuged at $5000 \times g$ for 10 min. The supernatants from these HuSaV-positive stool suspensions were aliquoted into individual tubes and stored at $-80^\circ C$ for subsequent use.

4.2 | Cell Lines

The human duodenal cancer cell line HuTu80 was purchased from ATCC and cultured in Iscove's Modified Dulbecco's Medium (IMDM; SIGMA) supplemented with 1% GlutaMAX-I (Gibco, Massachusetts, USA), 1% penicillin/streptomycin (Nacalai Tesque), and 5% heat-inactivated fetal bovine serum (FBS: CAPRICORN, Ebsdorfergrund, Germany).

The human embryonic kidney cell line HEK293T, maintained in our laboratory, was cultured in Dulbecco's modified eagle medium (DMEM; Nacalai Tesque) supplemented with 1% penicillin/streptomycin and 10% FBS.

The human colorectal adenocarcinoma cell line Caco-2 was purchased from ATCC and cultured in Minimum essential medium

(MEM; Nacalai Tesque) supplemented with 1% penicillin/streptomycin and 20% FBS.

The in-house maintained Caco-2/Cas9 cell line was cultured in MEM (Nacalai Tesque) supplemented with 1 mM Sodium Pyruvate (Nacalai Tesque), 1% MEM non-essential amino acids (Nacalai Tesque), 1% penicillin/streptomycin, and 10% FBS. HCT15 cells were cultured in Roswell Park Memorial Institute (RPMI)-1640 (Nacalai Tesque) supplemented with 1% penicillin/streptomycin and 10% FBS. HCT116 cells were cultured in McCoy's 5a Medium (Gibco) supplemented with 1% penicillin/streptomycin and 10% FBS. C2BBel cells were cultured in DMEM supplemented with 0.01 mg/mL human transferrin (Nacalai Tesque), 1% penicillin/streptomycin, and 10% FBS. All cell lines were cultured at 37°C with 5% CO₂ in a cell culture incubator.

4.3 | Supplements for the HuSaV Culture Trials

GCA (Nacalai Tesque), GCDCA (Sigma), and porcine bile (Sigma) were used as supplements for the HuSaV culture trials. Each supplement was dissolved in distilled water, filtered through a 0.22-μm pore size Millex-HV Syringe Filter Unit (Merck Millipore, Massachusetts, USA), and stored at 4°C.

4.4 | Screening Cell Lines for Susceptibility to HuSaV Infection

To evaluate the susceptibility of various cell lines to HuSaV, confluent cells were infected with a HuSaV GI.1 (AH20)-positive stool suspension, and the HuSaV RNA copy number in the culture supernatants was quantified via RT-qPCR. The medium used for the infections was modified: IMDM with 5% FBS was reduced to 3% FBS, and DMEM and MEM were reduced from 10% to 2% FBS. The HuSaV-positive stool suspension was filtered using a 0.45-μm pore Millex-HV Syringe Filter Unit. Based on a previous study (Takagi et al. 2020), 1000 μM GCA was added to the filtered stool suspension and medium mixture.

The experiments were conducted in 96-well plates. HuTu80 and HEK293T cells were inoculated with 1 μL of the stool suspension and 50 μL of medium and incubated at 37°C with 5% CO₂ for 24 h. Caco-2, HCT15, HCT116, Caco-2/Cas9, and C2BBel cells were inoculated with 0.05 μL of stool suspension and 50 μL of medium and incubated at 37°C with 5% CO₂ for 3 h. Cells were washed thrice with D-PBS (–), treated with 100 μL of medium containing 1000 μM GCA, and incubated at 37°C with 5% CO₂. The HuSaV RNA copy numbers in the culture supernatants were quantified at 0 or 1 dpi (immediately after medium replacement) and 7 dpi.

4.5 | Serial Passage of HuSaV GI.1 Using Culture Supernatants

HuTu80, HEK293T, Caco-2, and Caco-2/Cas9 cells were infected with a HuSaV GI.1 (AH20)-positive stool suspension. Each sample obtained from the initial infection was designated as Passage 0 (P + 0).

The experiments were conducted in 6-well plates. Cells were inoculated with 10 μL of stool suspension and 1 mL of medium and incubated at 37°C with 5% CO₂. HuTu80 and HEK293T cells were incubated for 24 h, while Caco-2 and Caco-2/Cas9 cells were incubated for 3 h. Subsequently, cells were washed three times with D-PBS (–) and refed with 2 mL of medium containing 1000 μM GCA. Cells were further incubated at 37°C with 5% CO₂. Seven days post-infection, 500 μL of the culture supernatant was mixed with 500 μL of fresh medium and used to inoculate new cells. This process was repeated to Passage 5 (P + 5).

4.6 | Dynamics of HuSaV RNA Copy Numbers and Infectivity Following HuSaV Infection

Caco-2MC cells were seeded in 24-well plates, and Passage 1 (P + 1) HuSaV GI.1 (M13-18) stock was utilized. Next, 250 μL of viral suspension was applied to Caco-2MC cells at an MOI of 0.01 and incubated at 37°C with 5% CO₂ for 3 h. After washing the cells three times with D-PBS (–), 500 μL of medium containing 1000 μM GCA was added, and the cells were cultured at 37°C with 5% CO₂. Culture supernatants were collected at 3 h post-infection (immediately after washing), and at 1, 2, 3, 4, 5, 6, and 7 dpi. The remaining cells were treated with 500 μL of distilled water and subjected to freeze–thaw cycles at –80°C thrice. Cell lysates were obtained by centrifuging at 10,000×g for 10 min. The HuSaV RNA copy numbers and TCID₅₀ were measured in the culture supernatants and cell lysates.

4.7 | Serial Passaging of HuSaV Genotypes GI.1, GI.2, GI.3, GII.1, GII.3, GIV.1, and GV.1 Using Cell Lysates

Caco-2MC cells were seeded in 12-well plates and inoculated with 50 μL of HuSaV-positive stool suspensions as to the following strains: GI.1 (M13-18, Ni17-9, and E22-22), GI.2 (M13-6), GI.3 (I21-042), GII.1 (TKC19-5 and TKC19-10), GII.3 (I22-124), GIV.1 (IB-02 and KA-31), and GV.1 (EH-40 and IB-24), and then 450 μL of medium was added to each well and incubated at 37°C with 5% CO₂ for 3 h. The culture supernatant was removed, and 1 mL of DW was added to extract the virus as previously described (0 dpi). In a separate plate, after incubation, cells were washed three times with D-PBS (–), and 1 mL of medium containing 1000 μM GCA was added. Cells were incubated at 37°C with 5% CO₂; at 5 dpi, the culture supernatant was removed, and 1 mL of DW was added to extract the virus. For GI.1, GI.2, and GI.3, the viruses were diluted in medium to achieve an MOI of 0.01, followed by inoculation with 500 μL of the prepared virus suspensions. For GII.1, GII.3, GIV.1, and GV.1, the RNA copy numbers were adjusted to that of HuSaV GI.1M13-18, with 500 μL added to each well. These virus suspensions were supplemented with 1000 μM GCA to infect Caco-2MC cells. The cells were incubated at 37°C with 5% CO₂ for 3 h. The same procedure was followed up to 5 dpi, with passaging carried out to Passage 2 (P + 2).

4.8 | Quantitative Reverse Transcription Polymerase Chain Reaction (RT-qPCR)

Viral RNA was quantified using single-step RT-qPCR with the Norovirus G1/G2 Detection Kit (TOYOBO, Osaka, Japan)

4.9 | Median Tissue Culture Infectious Dose (TCID₅₀) Assay

4.10 | Production and Purification of VLP

Large-scale VLP production was performed with High Five cells (1.6×10^8 cells) in a 200-mL culture volume, inoculated

4.11 | Preparation of GI.1 (AH20) Nonstructural Proteins

Genes to Cells, 2025

4.12 | Preparation of Anti-Serum Against VLP and Nonstructural Proteins

Rabbits and guinea pigs were immunized with purified VLPs, NS3, and NS7. Two immunizations were performed with a 4-week interval between doses, and sera were collected 10 days after the second immunization. All animal procedures were conducted by the Kiwa Institute for Experimental Animals (Wakayama, Japan).

4.13 | Immunofluorescence Assay

Virus-infected cells were washed twice with D-PBS (–) and fixed in 4% paraformaldehyde for 15 min. The cells were washed twice and permeabilized with 0.1% Triton X-100 in D-PBS (–) for 15 min at room temperature. After washing, the cells were blocked with 1% bovine serum albumin (BSA) in D-PBS (–) for 60 min at room temperature. For immunostaining, the cells were incubated with primary antibodies (1:1000 dilution)—rabbit or guinea pig anti-SaV VP1 hyperimmune serum raised against GI.1 AH20 VLPs, or rabbit hyperimmune serum raised against AH20 NS3 or NS7—for 60 min at 37°C. After washing, an Alexa Fluor 488- or 594-conjugated goat anti-rabbit or guinea pig secondary antibody (1:5000 dilution for VP1, 1:1000 dilution for NS3 and NS7; Invitrogen) was applied for 30 min at room temperature in the dark. Hoechst 33342 dye was used to stain the nuclei (1:10,000 dilution). The cells were visualized using a BZ-X810 imaging system (Keyence, Osaka, Japan).

4.14 | Flow Cytometry

After removing the culture supernatant, cells infected with HuSaV GI.1 for 4 days were washed with D-PBS (–) and detached using 0.5 g/L Trypsin-0.53 mmol/L EDTA (Nacalai Tesque) for 10 min. The cells were pelleted by centrifugation, fixed with 4% formaldehyde for 15 min, and permeabilized with methanol for 10 min at 4°C using the Intra Cellular Flow Cytometry kit (Cell Signaling Technology, MA, USA). After blocking with 1% BSA in D-PBS (–) for 60 min, the cells were incubated with guinea pig anti-HuSaV VLP serum (1:1000 dilution) overnight at 4°C. Following three washes, Alexa Fluor 488 goat anti-guinea pig IgG (1:1000 dilution) was applied for 60 min at room temperature. After washing, the cells were filtered through Falcon 5 mL Polystyrene Round-Bottom Tubes with 35 µm cell-strainer caps (Corning, New York, USA) and analyzed using a BD FACSMelody Cell Sorter (BD Biosciences, California, USA). Data analysis was performed using FlowJo software (BD Biosciences).

4.15 | Purification of Virus Particles

Caco-2/Cas9 cells were seeded onto 20 T75 flasks, infected with HuSaV GI.1 (AH20) at an MOI of 0.01, and incubated at 37°C for 7 days. The cells and culture supernatant (200 mL) were then collected using a cell scraper and centrifuged at 7000×g for 10 min. The supernatant was subjected to centrifugation over a

30% (w/v) sucrose cushion at 174,900×g for 2 h using an SW 32 Ti rotor (Beckman Coulter) (referred to as “culture supernatant” in the Results section). The pellet was resuspended in FBS-free MEM containing 0.5% ZWITTERGENT 3–14 (Merck Millipore, MA, USA), followed by centrifugation at 15,000×g for 10 min. The resulting supernatant was subjected to another sucrose cushion centrifugation (referred to as “cell lysate” in the Results section). After sucrose cushion centrifugation, the pellet from the culture supernatant was resuspended in FBS-free MEM, while the pellet from the cell lysate was resuspended in FBS-free MEM with ZWITTERGENT. Following resuspension, both samples were centrifuged at 15,000×g for 10 min. The supernatants were processed by CsCl density-gradient ultracentrifugation at 148,900×g for 24 h using an SW 55 Ti rotor (Beckman Coulter) and divided into 12 fractions. Each fraction was concentrated by ultracentrifugation at 367,600×g for 2 h using the SW 55 Ti rotor. The pellets were resuspended in FBS-free MEM. Virus particles were visualized by transmission electron microscopy (HT7700; Hitachi High Technologies, Tokyo, Japan). Purified virus samples were used for western blotting and infection assays.

4.16 | Western Blotting

Samples were mixed with sodium dodecyl sulfate (SDS) sample buffer and denatured at 100°C for 10 min. Proteins were separated by SDS-PAGE using 5%–20% e-PAGEL (ATTO, Tokyo, Japan) and transferred to a polyvinylidene difluoride (PVDF) membrane (Bio-Rad, California, USA) using a Trans-Blot Turbo system (Bio-Rad). The membrane was blocked with PVDF Blocking Reagent (TOYOBO) for 60 min, washed with D-PBS containing 0.05% Tween-20 (PBS-T), and incubated with the primary antibody guinea pig anti-HuSaV VLP antibody (1:1000 dilution in Can Get Signal Immunoreaction Enhancer Solution 1, TOYOBO) for 60 min at room temperature. After washing, the membrane was incubated with a goat anti-guinea pig IgG HRP secondary antibody (Abcam, Cambridge, UK), diluted 1:10,000 in Can Get Signal Immunoreaction Enhancer Solution 2 (TOYOBO) for 60 min at room temperature. Protein bands were visualized using Chemi-Lumi One L Solution A/B (Nacalai Tesque) and imaged with a ChemiDoc Touch system (Bio-Rad).

4.17 | Neutralization Assay

Caco-2MC cells were seeded on 96-well plates at 2×10^4 cells per well. Five-fold serial dilutions of rabbit anti-VLP antiserum and serum from a naïve rabbit were made (from $1:5^5$ to $1:5^{12}$). Twenty-five µL of AH20 containing 50 TCID₅₀ was mixed with each serum dilution, and then the mixture was incubated at 37°C for 2 h, followed by overnight incubation at 4°C. Subsequently, 50 µL of the virus-antiserum mixture was added to the cells and incubated at 37°C for 3 h. The medium was replaced with 100 µL of fresh medium containing 1000 µM GCA, and the cells were further incubated at 37°C. Next, HuSaV RNA copy numbers in the culture supernatant and cell lysates at 5 dpi were measured using RT-qPCR to assess the neutralization efficacy. Cell lysates were prepared by discarding the culture supernatant, adding 100 µL of DW to the cells, and subjecting the mixture to three freeze–thaw cycles at –80°C.

4.18 | Viral Genome Sequencing

Viral RNA was extracted from a 10% stool suspension or post-infection culture supernatant using the High Pure Viral RNA Kit (Roche) according to the manufacturer's instructions. Next-generation sequencing (NGS) was performed as described previously (Dennis et al. 2014). Briefly, a 200-bp fragment library was constructed for each sample with the NEBNext Ultra II RNA Library Prep Kit for Illumina v4.0 (New England Biolabs, Ipswich, MA, USA), according to the manufacturer's instructions. Each library was purified with Agencourt AMPure XP magnetic beads (Beckman Coulter). The DNA concentrations were determined with a Qubit 4 fluorometer and the Qubit dsDNA HS Assay Kit (Invitrogen). A 151-cycle paired-end-read sequencing run was conducted on an iSeq 100 desktop sequencer (Illumina, San Diego, CA, USA) with the iSeq 100 Reagent Kit v2 (300 cycles). The sequence data were analyzed with the CLC Genomics Workbench v8.0.2 (CLC Bio, Aarhus, Denmark). In this study, the nucleotide sequences of HuSaV strains AH20, M13-18, Ni17-9, E22-22, M13-6, I21-042, TKC19-5, TKC19-10, and I22-124 were newly determined using NGS and deposited in the GenBank/EMBL/DBJ databases under accession numbers LC671561, LC842313, LC842317, LC842321–LC842325, and LC842327.

Author Contributions

Yuya Fukuda: conceptualization, methodology, data curation, investigation, validation, formal analysis, visualization, resources, writing – original draft, writing – review and editing. **Azusa Ishikawa:** methodology, data curation, investigation, validation, formal analysis, visualization, writing – review and editing. **Ryoka Ishiyama:** data curation, methodology, investigation, validation, formal analysis, writing – review and editing. **Reiko Takai-Todaka:** conceptualization, supervision, project administration, writing – review and editing, resources. **Kei Haga:** conceptualization, methodology, data curation, investigation, validation, formal analysis, supervision, funding acquisition, project administration, resources, writing – review and editing. **Yuichi Someya:** data curation, formal analysis, investigation, methodology, validation, writing – review and editing. **Tomomi Kimura-Someya:** data curation, formal analysis, investigation, methodology, validation, writing – review and editing. **Kazuhiko Katayama:** conceptualization, methodology, data curation, investigation, formal analysis, supervision, funding acquisition, project administration, resources, writing – review and editing.

Acknowledgments

We would like to express our sincere gratitude to Prof. T. Tsugawa (Department of Pediatrics, Sapporo Medical University School of Medicine), Prof. H. Kimura (School of Medical Technology, Faculty of Health Sciences, Gunma Paz University), Dr. Y.H. Doan (Center for Emergency Preparedness and Response, National Institute of Infectious Diseases), and all individuals who contributed to the collection of stool samples. We extend our thanks to Dr. M. Kataoka (Department of Pathology, National Institute of Infectious Diseases) for her assistance in observing the virus through electron microscopy. We would like to thank Editage (<http://www.editage.com>) for editing and reviewing this manuscript for the English language.

Ethics Statement

This study was approved by the Ethics Committee of Kitasato Institute Hospital Research (Institutional ethical clearance number: 19476)

and the National Institute of Infectious Diseases (Institutional ethical clearance number: 532, 601, 802, and 1725). All procedures performed in studies involving human participants were in accordance with the ethical standards of the institutional and/or national research committee(s) and with the Helsinki Declaration (as revised in 2013). Informed consent was obtained in the form of opt-out on the website.

Conflicts of Interest

The authors declare no conflicts of interest.

Data Availability Statement

The data that support the findings of this study are available on request from the corresponding author. The data are not publicly available due to privacy or ethical restrictions.

References

- Becker-Dreps, S., F. Bucardo, and J. Vinjé. 2019. "Sapovirus: An Important Cause of Acute Gastroenteritis in Children." *Lancet Child & Adolescent Health* 3, no. 11: 758–759. [https://doi.org/10.1016/s2352-4642\(19\)30270-6](https://doi.org/10.1016/s2352-4642(19)30270-6).
- Chiba, S., S. Nakata, K. Numata-Kinoshita, and S. Honma. 2000. "Sapporo Virus: History and Recent Findings." *Journal of Infectious Diseases* 181, no. s2: S303–S308. <https://doi.org/10.1086/315574>.
- Chiba, S., Y. Sakuma, R. Kogasaka, et al. 1979. "An Outbreak of Gastroenteritis Associated With Calicivirus in an Infant Home." *Journal of Medical Virology* 4, no. 4: 249–254. <https://doi.org/10.1002/jmv.1890040402>.
- Dennis, F. E., Y. Fujii, K. Haga, et al. 2014. "Identification of Novel Ghanaian G8P[6] Human-Bovine Reassortant Rotavirus Strain by Next Generation Sequencing." *PLoS One* 9, no. 6: e100699. <https://doi.org/10.1371/journal.pone.0100699>.
- Diez-Valcarce, M., C. J. Castro, R. L. Marine, et al. 2018. "Genetic Diversity of Human Sapovirus Across the Americas." *Journal of Clinical Virology* 104: 65–72. <https://doi.org/10.1016/j.jcv.2018.05.003>.
- Doan, Y. H., Y. Yamashita, H. Shinomiya, et al. 2023. "Distribution of Human Sapovirus Strain Genotypes Over the Last Four Decades in Japan: A Global Perspective." *Japanese Journal of Infectious Diseases* 76, no. 4: 255–258. <https://doi.org/10.7883/yoken.jjid.2022.704>.
- Engle, M. J., G. S. Goetz, and D. H. Alpers. 1998. "Caco-2 Cells Express a Combination of Colonocyte and Enterocyte Phenotypes." *Journal of Cellular Physiology* 174, no. 3: 362–369. [https://doi.org/10.1002/\(sici\)1097-4652\(199803\)174:3%3C362::aid-jcp10%3E3.0.co;2-b](https://doi.org/10.1002/(sici)1097-4652(199803)174:3%3C362::aid-jcp10%3E3.0.co;2-b).
- Euller-Nicolas, G., C. L. Mennec, J. Schaeffer, et al. 2023. "Human Sapovirus Replication in Human Intestinal Enteroids." *Journal of Virology* 97, no. 4: e00383-23. <https://doi.org/10.1128/jvi.00383-23>.
- Fogh, J., W. C. Wright, and J. D. Loveless. 1977. "Absence of HeLa Cell Contamination in 169 Cell Lines Derived From Human Tumors." *Journal of the National Cancer Institute* 58, no. 2: 209–214. <https://doi.org/10.1093/jnci/58.2.209>.
- Guo, M., J. Hayes, K. O. Cho, A. V. Parwani, L. M. Lucas, and L. J. Saif. 2001. "Comparative Pathogenesis of Tissue Culture-Adapted and Wild-Type Cowden Porcine Enteric Calicivirus (PEC) in Gnotobiotic Pigs and Induction of Diarrhea by Intravenous Inoculation of Wild-Type PEC." *Journal of Virology* 75, no. 19: 9239–9251. <https://doi.org/10.1128/jvi.75.19.9239-9251.2001>.
- Haga, K., T. Tokui, K. Miyamoto, et al. 2024. "Neonatal Fc Receptor Is a Functional Receptor for Classical Human Astrovirus." *Genes to Cells* 29: 983–1001. <https://doi.org/10.1111/gtc.13160>.
- Hansman, G. S., K. Katayama, N. Maneekarn, et al. 2004. "Genetic Diversity of Norovirus and Sapovirus in Hospitalized Infants With

- Sporadic Cases of Acute Gastroenteritis in Chiang Mai, Thailand.” *Journal of Clinical Microbiology* 42, no. 3: 1305–1307. <https://doi.org/10.1128/jcm.42.3.1305-1307.2004>.
- Hassan, F., N. Kanwar, C. J., Harrison, et al. 2019. “Viral Etiology of Acute Gastroenteritis in < 2-year-old US Children in the Post-Rotavirus Vaccine Era.” *Journal of the Pediatric Infectious Diseases Society* 8, no. 5: 414–421.
- Hyde, J. L., S. V. Sosnovtsev, K. Y. Green, C. Wobus, H. W. Virgin, and J. M. Mackenzie. 2009. “Mouse Norovirus Replication Is Associated With Virus-Induced Vesicle Clusters Originating From Membranes Derived From the Secretory Pathway.” *Journal of Virology* 83, no. 19: 9709–9719. <https://doi.org/10.1128/jvi.00600-09>.
- Kapust, R. B., J. Tozser, J. D. Fox, et al. 2001. “Tobacco Etch Virus Protease: Mechanism of Autolysis and Rational Design of Stable Mutants With Wild-Type Catalytic Proficiency.” *Protein Engineering* 14, no. 12: 993–1000. <https://doi.org/10.1093/protein/14.12.993>.
- Lea, T. 2015. *Caco-2 Cell Line*, 103–111. Springer. https://doi.org/10.1007/978-3-319-16104-4_10.
- Li, T.-C., M. Kataoka, Y. H. Doan, et al. 2022. “Characterization of a Human Sapovirus Genotype GII.3 Strain Generated by a Reverse Genetics System: VP2 Is a Minor Structural Protein of the Virion.” *Viruses* 14, no. 8: 1649. <https://doi.org/10.3390/v14081649>.
- Lina, L., C. Saijuan, W. Chengyu, et al. 2019. “Adaptive Amino Acid Substitutions Enable Transmission of an H9N2 Avian Influenza Virus in Guinea Pigs.” *Scientific Reports* 9, no. 1: 19734. <https://doi.org/10.1038/s41598-019-56122-6>.
- Madeley, C. R. 1979. “Comparison of the Features of Astroviruses and Caliciviruses Seen in Samples of Feces by Electron Microscopy.” *Journal of Infectious Diseases* 139, no. 5: 519–523. <https://doi.org/10.1093/infdis/139.5.519>.
- Madeley, C. R., and B. P. Cosgrove. 1976. “Caliciviruses in Man.” *Lancet* 307, no. 7952: 199–200. [https://doi.org/10.1016/s0140-6736\(76\)91309-x](https://doi.org/10.1016/s0140-6736(76)91309-x).
- Matsumoto, N., S. Kurokawa, S. Tamiya, et al. 2023. “Replication of Human Sapovirus in Human-Induced Pluripotent Stem Cell-Derived Intestinal Epithelial Cells.” *Viruses* 15, no. 9: 1929. <https://doi.org/10.3390/v15091929>.
- Mautner, L., M. Hoyos, A. Dangel, C. Berger, A. Ehrhardt, and A. Baiker. 2022. “Replication Kinetics and Infectivity of SARS-CoV-2 Variants of Concern in Common Cell Culture Models.” *Virology Journal* 19, no. 1: 76. <https://doi.org/10.1186/s12985-022-01802-5>.
- Medici, M. C., F. Tummo, V. Albonetti, L. A. Abelli, C. Chezzi, and A. Calderaro. 2012. “Molecular Detection and Epidemiology of Astrovirus, Bocavirus, and Sapovirus in Italian Children Admitted to Hospital With Acute Gastroenteritis, 2008–2009.” *Journal of Medical Virology* 84, no. 4: 643–650. <https://doi.org/10.1002/jmv.23231>.
- Nakanishi, K., M. Tatsumi, K. Kinoshita-Numata, T. Tsugawa, S. Nakata, and H. Tsutsumi. 2011. “Full Sequence Analysis of the Original Sapporo Virus.” *Microbiology and Immunology* 55, no. 9: 657–660. <https://doi.org/10.1111/j.1348-0421.2011.00358.x>.
- Nakata, S., S. Honma, K. K. Numata, et al. 2000. “Members of the Family Caliciviridae (Norwalk virus and Sapporo virus) are the Most Prevalent Cause of Gastroenteritis Outbreaks Among Infants in Japan.” *Journal of Infectious Diseases* 181, no. 6: 2029–2032.
- Numata, K., M. E. Hardy, S. Nakata, S. Chiba, and M. K. Estes. 1997. “Molecular Characterization of Morphologically Typical Human Calicivirus Sapporo.” *Archives of Virology* 142, no. 8: 1537–1552. <https://doi.org/10.1007/s007050050178>.
- Oka, T., G. T. Stoltzfus, C. Zhu, K. Jung, Q. Wang, and L. J. Saif. 2018. “Attempts to Grow Human Noroviruses, a Sapovirus, and a Bovine Norovirus In Vitro.” *PLoS One* 13, no. 2: e0178157. <https://doi.org/10.1371/journal.pone.0178157>.
- Oka, T., T.-C. Li, K. Yonemitsu, et al. 2024. “Propagating and Banking Genetically Diverse Human Sapovirus Strains Using a Human Duodenal Cell Line: Investigating Antigenic Differences Between Strains.” *Journal of Virology* 98, no. 9: e0063924. <https://doi.org/10.1128/jvi.00639-24>.
- Pang, X. L., S. Honma, S. Nakata, and T. Vesikari. 2000. “Human Caliciviruses in Acute Gastroenteritis of Young Children in the Community.” *Journal of Infectious Diseases* 181, no. s2: S288–S294. <https://doi.org/10.1086/315590>.
- Park, S., S. Oh, S. Cho, et al. 2015. “Genetic Characterization of Sapovirus Detected in Hospitalized Children With Acute Gastroenteritis in Korea.” *Clinical Laboratory* 58, no. 11–12: 1219–1224. <https://pubmed.ncbi.nlm.nih.gov/23289192/>.
- Reed, L. J., and H. Muench. 1938. “A Simple Method of Estimating Fifty Percent Endpoints.” *American Journal of Epidemiology* 27, no. 3: 493–497. <https://doi.org/10.1093/oxfordjournals.aje.a118408>.
- Sakai, Y., S. Nakata, S. Honma, M. Tatsumi, K. Numata-Kinoshita, and S. Chiba. 2001. “Clinical Severity of Norwalk Virus and Sapporo Virus Gastroenteritis in Children in Hokkaido, Japan.” *Pediatric Infectious Disease Journal* 20, no. 9: 849–853. <https://doi.org/10.1097/00006454-200109000-00005>.
- Sánchez, G. J., H. Mayta, M. J. Pajuelo, et al. 2017. “Epidemiology of Sapovirus Infections in a Birth Cohort in Peru.” *Clinical Infectious Diseases* 66, no. 12: 1858–1863. <https://doi.org/10.1093/cid/cix1103>.
- Suzuki, H., T. Konno, T. Kutsuzawa, et al. 1979. “The Occurrence of Calicivirus in Infants With Acute Gastroenteritis.” *Journal of Medical Virology* 4, no. 4: 321–326. <https://doi.org/10.1002/jmv.1890040410>.
- Takagi, H., T. Oka, T. Shimoike, et al. 2020. “Human Sapovirus Propagation in Human Cell Lines Supplemented With Bile Acids.” *Proceedings of the National Academy of Sciences* 117, no. 50: 32078–32085. <https://doi.org/10.1073/pnas.2007310117>.
- Terashima, H., S. Chiba, Y. Sakuma, et al. 1983. “The Polypeptide of a Human Calicivirus.” *Archives of Virology* 78, no. 1–2: 1–7. <https://doi.org/10.1007/bf01310853>.

Supporting Information

Additional supporting information can be found online in the Supporting Information section.